

# Fault Diagnosis and Noise Robustness Comparison of Rotating Machinery using DWT and Artificial Neural Networks

Jongkyu Lee, Donghee Lee, Byeongwoo Kim\*

*Department of Electrical Engineering, University of Ulsan 93 Daehak-ro,  
Mugeo-Dong, Nam-Gu, Ulsan, South Korea.*

## Abstract

For systems using rotating machinery, diagnosing the faults of the rotating machinery is critical for system maintenance. Recently, a machine-learning algorithm has been employed as one of the methods for diagnosing the faults of rotating machinery. This algorithm has the advantage of automatically classifying faults without an expert knowledge. However, despite a good training performance of the machine-learning model, there remains a challenge of performance degradation arising from noise when the model is applied in a real environment. In this study, to solve this problem, we identified the faults of a rotating machinery after applying the discrete wavelet transform. We extracted the feature parameters useful for detecting the faults of rotating machinery and applied them to the artificial neural network. Subsequently, we compared it with a commonly used signal-analysis technique and matched the feature importance according to load and noise. We verified that the proposed method improved the performance in diagnosing the faults of rotating machinery.

**Keywords:** Rolling bearing fault diagnosis, Discrete wavelet transform, Feature extraction, Feature importance

## I. INTRODUCTION

With industrial development and technological advances, various types of industrial rotating machinery have been subjected to high speed and heavy loads. This puts lots of mechanical and thermal stresses on rotating machinery, causing them to fail [1]. Diagnosing the faults of rotating machinery is critical because significant time/economic losses occur when there is an abnormality in rotating machinery. Therefore, there is a need for countermeasures to check the state of rotating machinery and diagnose the faults. According to statistical data, 45–55% of malfunctions in rotating machinery are attributed to faults in bearings [2]. It is crucial to monitor the state of rotating machinery to reduce the loss by diagnosing the malfunctions of rotating machinery in advance [3] [4] [5].

To obtain signals indicating the state of rotating machinery, sound meters, motor current signals, and vibration signals are mainly used [7][8][9]. Vibration sensors are predominant since

they are easy to measure and indicate the state of rotating machinery [10].

Generally, fault diagnosis of rotating machinery is composed of two stages: the feature extraction of vibration signals and classification of the fault state of rotating machinery using the extracted features [11] [12] [13] [14].

The vibration signal measured in rotating machinery appears as a mixture of vibration and noise signals that indicate the state of rotating machinery. Supposing the vibration signal containing noise is used as the input value of the machine learning model, the noise makes it difficult to accurately diagnose the state of rotating machinery. Consequently, it is essential to remove the noise signal from the vibration signal and extract only the vibration signal indicating the fault state. This process is called the feature point extraction.

The common way of extracting feature points is to use filters and signal decomposition [15] [16] [17]. As the most typical ways of diagnosing faults in the vibration signal, we have the empirical mode decomposition (EMD) that decomposes the signal using the intrinsic mode function (IMF). and the wavelet transform that decomposes the signal using the wavelet function.

The EMD technique detects faults by decomposing the vibration signal into several sub-bands using IMF and then extracting feature points from the decomposed sub-bands [18]. The EMD technique shows excellent performance when detecting faults in the vibration signal [19]. However, the sub-bands decomposed by IMF are not orthogonal to each other, thus combining the signals is inevitable.

The wavelet transform method decomposes the vibration signal into sub-bands by applying a wavelet function to the signal and then extracting feature points from the decomposed sub-bands [20]. The wavelet function has the advantage of displaying feature points clearly by controlling the period and amplitude, as well as reducing noise during the wavelet transform [21].

After extracting feature points from a vibration signal, the state of rotating machinery is represented using the extracted feature points; this process is known as fault state classification.

Machine-learning algorithm is the prevalent method used to classify the faults of the rotating machinery. It uses the feature points extracted from the rotating machinery as input values. The machine learning algorithm trains itself based on the data used as input values to classify the state of machinery.

We decomposed the vibration signal by using the discrete wavelet transform, which was one of the wavelet transforms, to detect the faults of rotating machinery, as well as extracted parameters useful for detecting the faults of rotating machinery in the decomposed signal. The fault state of rotating machinery was classified using the extracted feature points as input values of the artificial neural network, which was one of the machine-learning algorithms. In addition, to confirm the performance of the discrete wavelet transform, we verified its usefulness by comparing it with the conventional method by adding white Gaussian noise [22].

## II. THEORY

### Discrete wavelet transform

Contrary to the Fourier transform that does not exhibit the characteristics of the aperiodic signal efficiently due to fixed resolution, the wavelet transform can analyze the vibration signal using the wavelet function with fluid resolution. This is referred as continuous wavelet transform (CWT). CWT is calculated as follows.

$$CWT(a, b) = \int_{\mathbb{R}} x(t) \frac{1}{\sqrt{a}} \psi^*\left(\frac{t-b}{a}\right) dt \quad (1)$$

As in Equation (1), the wavelet function  $\psi(t)$  such as morlet, coiflet, haar, or symmlet, that can separate the aperiodic signal is defined. This wavelet function is shifted by  $b$  on the time axis and scaled by  $a$  to decompose the signal. Here,  $\psi^*(t)$  is the dot product of the wavelet function. The wavelet function is composed of a set of functions with different periods, and this characteristic enables multi-resolution decomposition.

When analyzing the vibration signal, CWT contains unnecessary data due to high redundancy in the signal, resulting in a high risk of errors, as well as lengthening the computational process. To address these drawbacks, parameters  $a$  and  $b$  are defined in the DWT as follows.

$$a = 2^j, j \in \mathbb{Z} \quad (2)$$

$$b = k2^j, j, k \in \mathbb{Z} \quad (3)$$

The DWT is defined as follows by the changed parameters.

$$DWT(j, k) = 2^{-\frac{j}{2}} \int_{\mathbb{R}} x(t) \frac{1}{\sqrt{a}} \psi^*(2^{-j}t - k) dt \quad (4)$$

Through this process, the original CWT becomes the discrete wavelet function and the scaling function.

$$\psi_{j,k}(t) = 2^{-\frac{j}{2}} \psi(2^{-j}t - k) \quad (5)$$

$$\phi_{j,k}(t) = 2^{-\frac{j}{2}} \phi(2^{-j}t - k) \quad (6)$$

When analyzing the vibration signal using the DWT, the wavelet coefficient of the vibration signal can be obtained as follows.

$$a_{2^j}(k) = \int x(t) \phi_{j,k}(t) dt \quad (7)$$

$$d_{2^j}(k) = \int x(t) \psi_{j,k}^*(t) dt \quad (8)$$

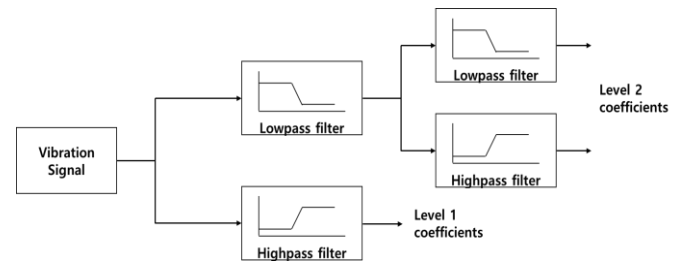


Fig 1. Signal filtering process of DWT

Through Equation (7) and (8), we observe that the signal is decomposed into approximations and details.

The discrete wavelet function and scaling function act as a low-frequency pass filter and a high-frequency pass filter, respectively. From Fig. 1, approximations have a low-frequency resolution, whereas details have a high frequency resolution.

### Artificial neural network

In machine learning, an artificial neural network mathematically imitates the structure of biological neurons. The structure of the artificial neural network is composed of an input layer, a hidden layer, and an output layer. A layer is composed of several nodes. The output value is represented by calculating the weight of each node and the input value, which is expressed as (9).

$$Z_i(X) = \sum_i^n w_i x_i + b \quad \text{for } i = 1, 2, \dots, n \quad (9)$$

$Z_i$  refers to the output value,  $w_i$  to the weight,  $x_i$  to the input value,  $b$  to the bias, and  $n$  to the number of nodes.

The final value calculated in (9) is substituted into the activation function whose result is finally used for fault classification. The activation function is applied to (10).

$$\bar{Y} = h(Z) \quad (10)$$

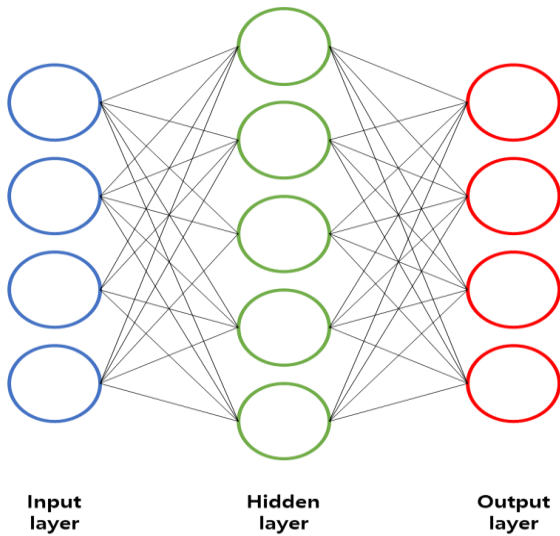


Fig 2. Structure of artificial neural network

$$entropy = - \sum_{x=1}^N P(x) \log P(x) \quad (13)$$

$$variance = \frac{1}{N-1} \sum_{i=1}^N |x_i - \mu|^2 \quad (14)$$

$$peak = \max(x_i) \quad (15)$$

$$kurtosis = \frac{1}{N} \sum_{i=1}^N |x_i|^4 \quad (16)$$

$$skewness = \frac{1}{N} \sum_{i=1}^N \frac{x_i - \bar{x}}{\sigma} \quad (17)$$

### III. EXPERIMENT SETUP

#### Data processing

In this paper, constructing various datasets is required to improve the accuracy of the fault diagnosis of rotating machinery. Accordingly, we used the Case Western Reserve University Bearing Fault database, which is frequently utilized in relation to the conventional fault diagnosis of rotary machinery [23]. Since many researchers have conducted experiments with these data, they are reliable and have the advantage of comparing the performance with other learning

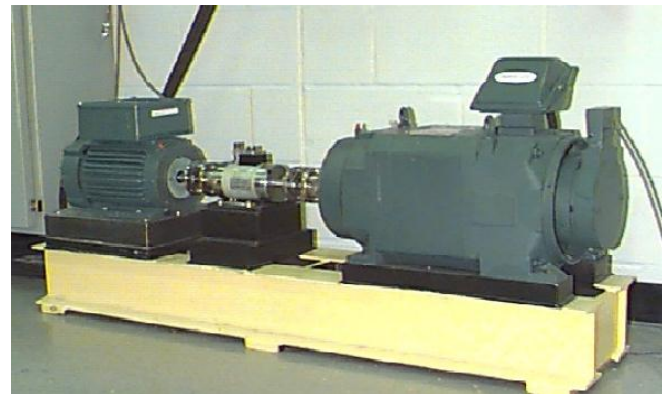


Fig 4. Representation of proposed fault diagnosis structure in neural network

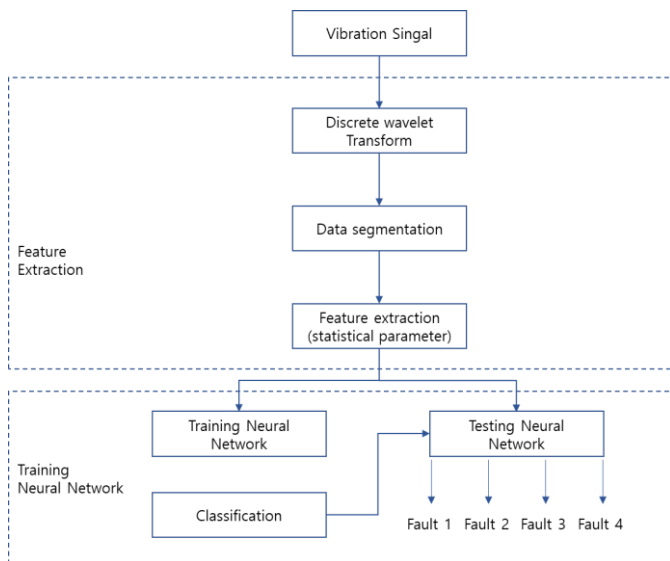


Fig 3. Experiment setup

value to confirm whether the artificial neural network accurately predicts the result value, which is (11).

$$error = y_{target} - y_{predict} \quad (11)$$

$y_{target}$  is the actual value and  $y_{predict}$  is the result predicted by the artificial neural network. By comparing these two values, the artificial neural network is trained to minimize errors.

#### Feature extraction

Feature point extraction crucially influences the fault diagnosis of rotating machinery. The best way to diagnose the faults of rotating machinery from the vibration signal is to utilize the statistical parameters of the vibration signal. The statistical parameters we present are as follows.

$$rms = \sqrt{\frac{1}{N} \sum_{i=1}^N |x_i|^2} \quad (12)$$

advantage of comparing the performance with other learning algorithms. As seen in Fig. 3, the test bench consists of a motor in the left, a torque transducer/encoder in the middle, and a dynamometer in the right. The vibration signal was measured in four types as follows: normal, ball fault, outer ring fault, and inner ring fault. The degree of crack has values 0.007, 0.014, and 0.021 inch, and the load stage has values of 0 HP, 1 HP, 2 HP, 3 HP.

We presented the process of diagnosing the faults of rotating machinery using the vibration signal as shown in Fig. 4.

We also utilized data with a crack of 0.007 inch and classified data sets into Case 1 (= 0 HP), Case 2 (= 1 HP), Case 3 (= 2 HP), and Case 4 (= 3 HP) based on the degree of load. Each case consisted of 4368 data (normal = 1092, ball fault = 1092, outer ring fault = 1092, and inner ring fault = 1092). In addition, when analyzing the vibration signal, we increased the white Gaussian noise in the vibration signal with a crack of 0.007 inch to verify the robustness to noise in the discrete wavelet transform. As shown in Fig. 5, we constructed the sample data to train the artificial neural network by segmenting the actual

vibration signal added with white Gaussian noise into 4392. For each sample data, we applied Daubechies wavelet 10, which was the discrete wavelet function. We then extracted the statistical parameters proposed to use as the input values of the artificial neural network in the approximation level 1 signal applied with the discrete wavelet transform.

**Create neural network**

To detect the faults of rotating machinery, the number of nodes in the input layer of the artificial neural network was set to 6 (i.e., rms, entropy, peak, variance, kurtosis, skewness), in the hidden layer to 20, and in the output layer to 4. This is because the four fault states required to be identified.

From the data sets of each case to train the artificial neural network, a train set accounted for 70%, a validation set to determine whether the training goes well accounted for 15%, and the remaining 15% was allocated to a test set to determine the performance of the entire artificial neural network. When training the artificial neural network, the activation function used the sigmoid function, the backpropagation used the scaled

training the artificial neural network, the activation function used the sigmoid function, the backpropagation used the scaled conjugated gradient, and the classification used the cross-entropy. In addition, we configured the system to forcefully terminate the training in case of any overfitting. During training, the artificial neural network using the validation was set to prevent overfitting. In this paper, to verify the robustness to noise of the discrete wavelet transform, we compared it with the conventional empirical mode decomposition (EMD) technique.

**IV. SIMULATION**

**Comparison accuracy & loss**

As illustrated in Fig. 4, after the DWT of the vibration signal was added to white Gaussian noise using Daubechies wavelet 10, which was the discrete wavelet function, we extracted the proposed statistical parameters and then used them as the input values of the artificial neural network.

To compare the performance of the generated artificial neural network (Fig. 6), we compared the accuracy and loss between DWT and EMD by SNR level. When the SNR was 1 dB in the

Case1 (= 0 HP) data set, the accuracy of the artificial neural network model using the DWT was 82.6% and the loss was 0.07782. This indicated a better performance than the vibration signal analysis method using the EMD technique. (IMF1 – accuracy: 70.1%, loss: 0.1538, IMF2 – accuracy: 71.2%, loss: 0.1488, IMF1+IMF2 – accuracy: 0.07781). In addition, when the noise was gradually reduced, the vibration signal analysis method using the DWT reached an accuracy of 100% when the SNR was 15 dB. In contrast, the vibration signal analysis method using the commonly used EMD technique did not reach an accuracy of 100% due to poor denoise performance. The loss performance was also degraded compared to the vibration signal analysis method using DWT. As shown in Fig. 6, we comparatively analyzed the performance of the artificial neural network by gradually increasing the load (Case 2 = 1 HP, Case 3 = 2 HP, Case 4 = 3 HP).

When the SNR was 1 dB, the accuracy of the artificial neural network model using the DWT was reduced compared to the no-load condition (Case 2 - accuracy: 71.7%, loss: 0.1388, Case 3 –accuracy: 71.9%, loss: 0.1431, Case 4 – accuracy: 69.3%, loss: 0.1411).

However, overall when the SNR was 17 dB, the accuracy reached 100% (Case 2 (17 dB) – accuracy: 100% loss: 0.001337, Case 3 (17 dB) – accuracy: 100%, loss: 0.001428, Case 4 (17 dB) – accuracy: 100%, loss: 0.000201), and the performance was better than in the vibration signal analysis method using the EMD technique (Case 2 (17 dB): IMF1 – accuracy: 90.7%, loss:

0.001149, IMF2 – accuracy: 90.6%, loss: 0.05915, IMF1+IMF2 – accuracy: 89.9%, loss: 0.06203, Case 3 (17 dB):

IMF1 – accuracy: 90.4%, loss: 0.05853, IMF2 – accuracy: 90.3%, loss: 0.05988, IMF1+IMF2 – accuracy: 89.5%, loss: 0.06088, Case 4 (17 dB): IMF1 – accuracy: 88%, loss: 0.0731, IMF2 – accuracy: 87.9%, loss: 0.07676, IMF1+IMF2 – accuracy: 88.1%, loss: 0.07942).

These results confirmed that the vibration signal analysis using the discrete wavelet transform showed an improved robustness to noise as compared to the conventional method. Furthermore, when we extracted the feature points and used them as the input values of the artificial neural network after applying the discrete wavelet transform, we confirmed the effectiveness and safety compared to the conventional vibration signal analysis method.

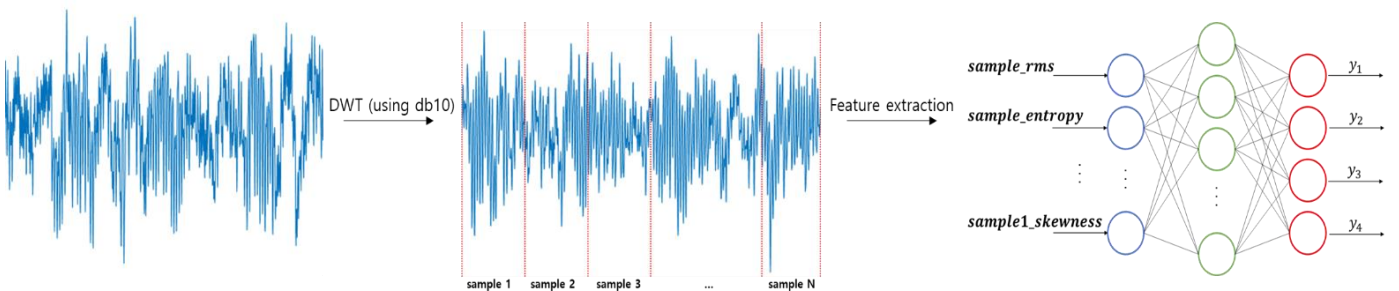


**Fig 4.** The process of fault diagnosis in vibration signal adding gaussian noise

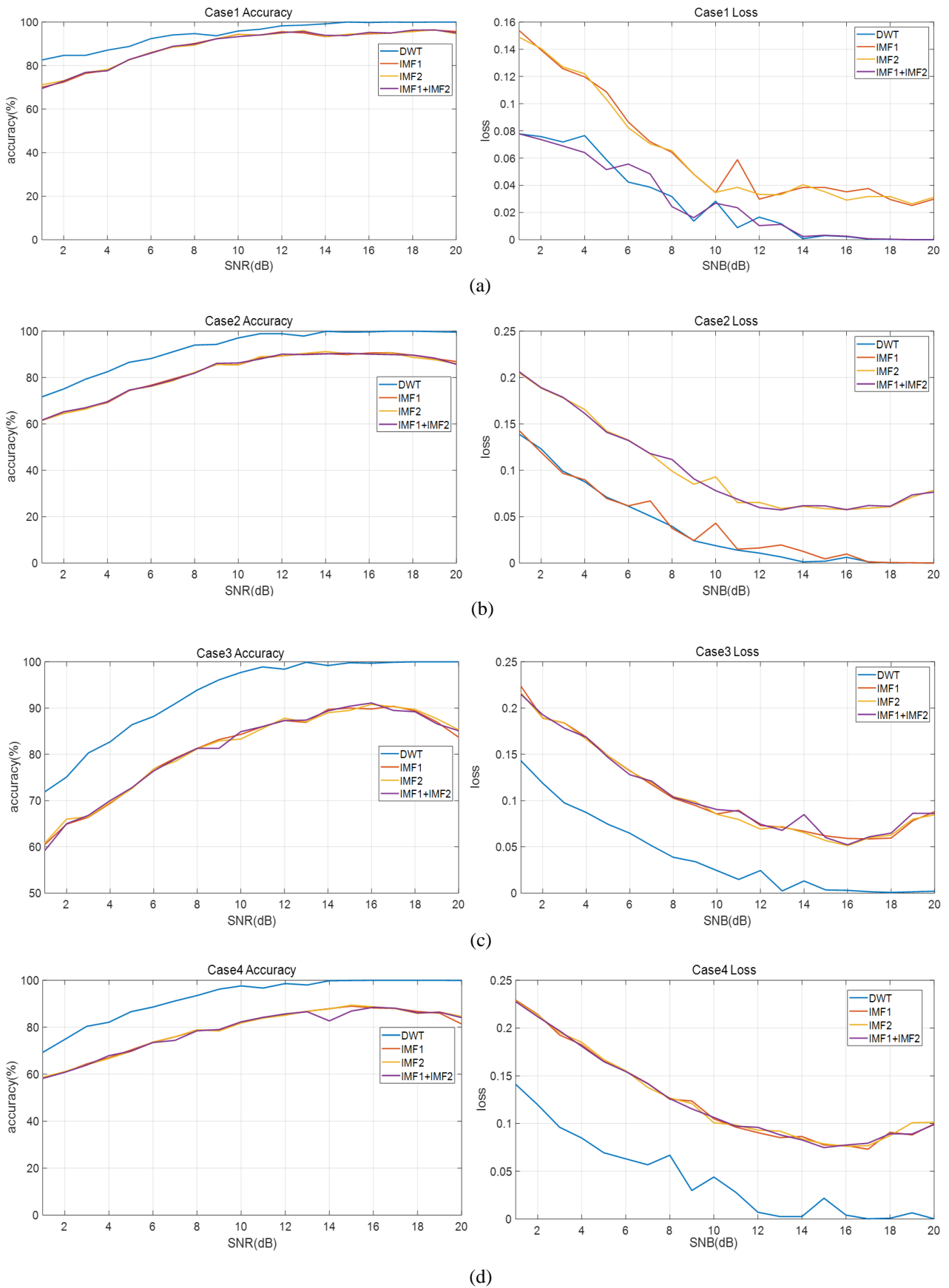


**Fig 5.** Result of fault diagnosis (accuracy & loss) – (a) Case1(=0HP) (b)Case2(=1HP) (c)Case3(=2HP) (d)Case4(=3HP)

**Feature importance of artificial neural network**

We displayed the results in Table 1 by using the weight connection algorithm to identify the importance of parameters according to load and noise in the fault diagnosis of rotating machinery using the vibration signal [24].

For Case 1, when SNR is 1, the artificial neural network performance is affected in the order of kurtosis, rms, variance, skewness, peak, and entropy; when SNR is 10, the performance is affected in the order of skewness, variance, peak, kurtosis, entropy, and rms; and when SNR is 20, the performance is affected in the order of peak, skewness, variance, entropy, kurtosis, and rms.

For Case 2, when SNR is 1, the artificial neural network performance is affected in the order of kurtosis, peak, variance, entropy, skewness, and rms; when SNR is 10, in the order of skewness, kurtosis, rms, entropy, and peak; and when SNR is 20, in the order of peak, rms, entropy, skewness, and variance.

For Case 3, when SNR is 1, the artificial neural network performance is affected in the order of rms, peak, kurtosis, entropy, variance, and skewness; when SNR is 10, in the order of rms, entropy, peak, kurtosis, skewness, and variance; and when SNR is 20, in the order of peak, skewness, variance, kurtosis, entropy, and rms.

For Case 4, when SNR is 1, the performance of the artificial neural network is affected in the order of *kurtosis, variance, entropy, peak, rms, and skewness*; when SNR is 10, in the order of variance, rms, peak, kurtosis, skewness, and entropy; and when SNR is 20, in the order of kurtosis, peak, entropy, variance, skewness, and rms.

The above results indicate that the degree of load does not significantly affect the feature importance of the artificial neural network. However, the intensity of noise affects the feature importance of the artificial neural network.

**Table 1.** Feature importance comparison by load and noise

	Input (SNR 1)	Weight connection	Rank	Input (SNR 10)	Weight Connection	Rank	Input (SNR 20)	Weight Connection	Rank
Case1	<i>peak</i>	1.3891	5	<i>peak</i>	-0.4600	3	<i>peak</i>	5.4696	1
	<i>entropy</i>	-6.8009	6	<i>entropy</i>	-9.4767	5	<i>entropy</i>	1.9053	4
	<i>skewness</i>	2.0257	4	<i>skewness</i>	5.9000	1	<i>skewness</i>	3.3109	2
	<i>kurtosis</i>	7.3396	1	<i>kurtosis</i>	-1.9693	4	<i>kurtosis</i>	-2.4286	5
	<i>variance</i>	4.5867	3	<i>variance</i>	0.2013	2	<i>variance</i>	2.8304	3
	<i>rms</i>	5.4010	2	<i>rms</i>	-27.9849	6	<i>rms</i>	-3.1797	6
Case2	<i>peak</i>	12.0866	2	<i>peak</i>	-2.9464	6	<i>peak</i>	8.3396	1
	<i>entropy</i>	9.4048	4	<i>entropy</i>	-1.6847	5	<i>entropy</i>	3.1561	3
	<i>skewness</i>	0.9414	5	<i>skewness</i>	5.3616	1	<i>skewness</i>	1.9339	5
	<i>kurtosis</i>	12.2516	1	<i>kurtosis</i>	-0.9151	3	<i>kurtosis</i>	2.4996	4
	<i>variance</i>	10.4544	3	<i>variance</i>	-0.7794	2	<i>variance</i>	0.6884	6
	<i>rms</i>	-1.5704	6	<i>rms</i>	-0.9560	4	<i>rms</i>	3.6871	2
Case3	<i>peak</i>	2.3758	2	<i>peak</i>	0.7677	3	<i>peak</i>	6.8431	1
	<i>entropy</i>	-0.0577	4	<i>entropy</i>	4.5048	2	<i>entropy</i>	-2.3311	5
	<i>skewness</i>	-5.9106	6	<i>skewness</i>	-3.3227	5	<i>skewness</i>	1.8187	2
	<i>kurtosis</i>	1.7786	3	<i>kurtosis</i>	-1.7910	4	<i>kurtosis</i>	-0.7298	4
	<i>variance</i>	-0.7305	5	<i>variance</i>	-3.4876	6	<i>variance</i>	0.9775	3
	<i>rms</i>	13.3524	1	<i>rms</i>	10.0270	1	<i>rms</i>	-5.1456	6

Case4	<i>peak</i>	-3.9757	4	<i>peak</i>	-0.3804	3	<i>peak</i>	4.9393	2
	<i>entropy</i>	-1.1748	3	<i>entropy</i>	-9.7355	6	<i>entropy</i>	4.4743	3
	<i>skewness</i>	-6.7264	6	<i>skewness</i>	-7.3626	5	<i>skewness</i>	-7.1037	5
	<i>kurtosis</i>	5.5924	1	<i>kurtosis</i>	-0.9376	4	<i>kurtosis</i>	8.5410	1
	<i>variance</i>	2.3544	2	<i>variance</i>	5.9906	1	<i>variance</i>	-7.1002	4
	<i>rms</i>	-4.2686	5	<i>rms</i>	5.3312	2	<i>rms</i>	-17.4795	6

## V. CONCLUSION

In this paper, we analyzed the vibration signal to diagnose the faults of rotating machinery. In addition, to investigate the robustness to noise, we gradually added white Gaussian noise to the vibration signal, and then extracted 6 statistical parameters used as the input values of the artificial neural network by applying the discrete wavelet transform.

The artificial neural network model using the vibration signal applied with a discrete wavelet was confirmed to achieve excellent accuracy as compared to the conventional signal analysis method. It showed the feature importance of statistical parameters according to noise and load. As a result, we were able to improve the inaccuracy caused by noise observed when measuring the vibration signal in a real environment, as well as show a change in feature importance caused by noise and load.

## VI. ACKNOWLEDGMENT

This research was supported by 2019 Industrial Employment Crisis Area Technology, "ESS Safety certification system for ships and international testing laboratory" (Grant Number: P075100005) and Market independent 3G xEV industry development business, "development of the systematization platform for expending the industry of xEV parts"(Grant Number: No.20010132)

## REFERENCE

- [1] A. H. Bonnett, G. C. Soukup, 1992, "Cause and analysis of stator and rotor failures in three-phase squirrel-cage induction motors", IEEE Transaction on Industry Applications, vol. 28, no 4, pp921-937
- [2] Nandi, S., Toliyat, H. A., & Li, X., 2005, "Condition monitoring and fault diagnosis of electrical motors – a review", IEEE Transactions on Instrumentation and Measurement, 65(11), pp.2646-2656
- [3] B. Dolenc, P. Boskoski, D.Juricic , 2016, "Distributed bearing fault diagnosis based on vibration analysis", Mech. Syst. Signal Process, 66-67, pp521-532
- [4] L. Barbini, A.J. Hillis, J.L. du Bois, 2018, "Amplitude-cyclic frequency decomposition of vibration signals for bearing fault diagnosis based on phase editing", Mech. Syst. Signal Process, 103, pp76-88
- [5] E. El-Thalji, Jantunen, 2015, "A summary of fault modeling and predictive health monitoring of rolling bearings", Mech. Syst. Signal Process, 60-61, pp252-272
- [6] Huang, D.-S & Du, J.-X. ,2008, "Systematic theory of neural networks for pattern recognition", Beijing 201: Publishing House of Electronic Industry of China.
- [7] Chacon, J.L.F., Kappatos, V., Balachandran, W., & Gan, T.-H., 2015 "A novel approach for incipient defect detection in rolling bearings using acoustic emission technique", Applied Acoustics, 89, pp88-100.
- [8] Singh, S., Kumar, A., & Kumar, N., 2014," Motor current signature analysis for bearing fault detection in mechanical system", Procedia Materials Science, 6, pp171-177
- [9] Zarei, J., Tajeddini, M. A., & Karimi, H. R., 2014, "Vibration analysis for bearing fault detection and classification using an intelligent filter", Mechatronics, 24(20), pp151-157
- [10] Kharche, P., P., & Ksgirsagar, S. V., 2014, "Review of fault detection in rolling element bearing", International Journal of Innovative Research in Advanced Engineering, 1(5), pp169-174
- [11] W.K. Xi, Z.X. Li, Z. Tian, et al.,2018, "A feature extraction and visualization method for fault detection of marine diesel engines", Measurement, 116, pp429-437
- [12] J.B. Yu, J.X Lv, 2017, "Weak fault feature extraction of rolling bearings using local mean decomposition-based multilayer hybrid denoising", IEEE Trans. Instrum. Meas., 66(12), pp3148-3159
- [13] M. Amar, I. Gondal, C. Wilson, 2015, "Vibration spectrum imaging: a novel bearing fault classification approach", IEEE Trans Ind. Electron., 51(1), pp494-502
- [14] B. Madahian, L.Y. Deng, R. Homayouni, 2015, "Development of a literature informed Bayesian machine learning method for feature extraction and classification", BMC Bioinform, 16.
- [15] W. He. Z.N. Jiang., K. Feng, 2009, "Bearing fault detection based on optimal wavelet filter and sparse code shrinkage", Measurement, 42(7), pp1092-1102

- [16] X. L. An, H. T. Zeng, W. W. Yang, et al., 2017, "Fault diagnosis of a wind turbine rolling bearing using adaptive local iterative filtering and singular value decomposition, T. I. Meas. Control., 39(11), pp1643-1648
- [17] Xueli An, Weiwei Yang, Xuemin An, 2017, "Vibration signal analysis of a hydropower unit based on adaptive local iterative filtering", P. I. Mech. Eng. C-J Mec. 231(7), pp1339-1353
- [18] Y. Li, M. Xu, X. Liang, 2017, "Huang Application of bandwidth EMD and adaptive multiscale morphology analysis for incipient fault diagnosis of rolling bearings", IEEE Trans. Ind. Electron., 61(8), pp6506-6517
- [19] J.P. Yang, P.Z. Li, Yang, et al., 2018, "An improved EMD method for modal identification and a combined static-dynamic method fir damage detection", Sound Vib., 240, pp242-260
- [20] Q.B. He, 2013, "Vibration signal classification by wavelet packet energy flow manifold learning", J. Sound Vib., 332(7), pp1881-1894
- [21] Q. Pan, L. Zhang, G. Dai, H. zhang, 1991"Two denoising methods by wavelet transform", IEEE Trans. Signal Processing, 47(12), pp 3401-3406
- [22] S. Li, W. Zhou, Q. Yaun, et al., "Feature extraction and recognition of ictal EEG using EMD and SVM"
- [23] Loparo, K. A., 2005," Bearing fault diagnosis based on wavelet transform and fuzzy inference.", Mechanical System and Signal Processing
- [24] Olden, J.D., Jackson, D.A., 2002, "Illuminating the "black box": understanding variable contributions in artificial neural networks.", Ecol. Model, 154, pp 135-150